Energy-Efficient Design of STAR-RIS Aided MIMO-NOMA Networks

Fang Fang, *Member, IEEE*, Bibo Wu, Shu Fu, *Member, IEEE*, Zhiguo Ding, *Fellow, IEEE*, and Xianbin Wang, *Fellow, IEEE*

***Abstract*— Simultaneous transmission and reflection-reconfigurable intelligent surface (STAR-RIS) can provide expanded coverage compared with the conventional reflection-only RIS. This paper exploits the energy efficient potential of STAR-RIS in a multiple-input and multiple-output (MIMO) enabled non-orthogonal multiple access (NOMA) system. Specifically, we mainly focus on energy-efficient resource allocation with MIMO technology in the STAR-RIS assisted NOMA network. To maximize the system energy efficiency, we propose an algorithm to optimize the transmit beamforming and the phases of the low-cost passive elements on the STAR-RIS alternatively until the convergence. Specifically, we first decompose the formulated energy efficiency problem into beamforming and phase shift optimization problems. To efficiently address the non-convex beamforming optimization problem, we exploit signal alignment and zero-forcing precoding methods in each user pair to decompose MIMO-NOMA channels into single-antenna NOMA channels. Then, the Dinkelbach approach and dual decomposition are utilized to optimize the beamforming vectors. In order to solve non-convex phase shift optimization problem, we propose a successive convex approximation (SCA) based method to efficiently obtain the optimized phase shift of STAR-RIS. Simulation results demonstrate that the proposed algorithm with NOMA technology can yield superior energy efficiency performance over the orthogonal multiple access (OMA) scheme and the random phase shift scheme.**

***Index Terms*— Energy efficiency, STAR-RIS, NOMA, MIMO, multiple user pairs.**

I. Introduction

THE reconfigurable meta-surface with a large number of low-cost elements is considered as a promising technology to enable defined radio environment in the future wireless network [1]. With the significantly increased radio frequencies and line-of-sight signal propagation, achieving desired signal coverage has become a major challenge for the the sixth generation (6G) mobile networks. In the traditional reconfigurable intelligent surface (RIS), an intelligent controller is attached to the RIS to alter the propagation of the reflected electromagnetic waves with desired direction, which is usually towards the intended user. Both the phase and even the amplitude of these reconfigurable elements can be adjusted to achieve user-defined radio propagation environment. Due to the low-cost elements of the RIS and passive operation without additional energy consumption, RIS has been regarded as a promising technology to address the issue of high energy consumption in 6G. There are two typical structures, i.e., Reconfigurable intelligent surface (RIS) [2], [3] and Simultaneous transmitting and reflecting reconfigurable intelligent surface (STAR-RIS) [4], [5]. Compared to the reflecting-only RIS, STAR-RIS can serve the users on both sides of the surface, located at its front and back by simultaneously transmitting and reflecting the incident signal. Non-orthogonal multiple access (NOMA) has been recognized as a promising physical layer technique in beyond fifth generation (B5G) and 6G to effectively improve spectral efficiency, support massive connectivity, and reduce transmission latency, etc. The key idea of NOMA is to exploit the controlled non-orthogonality and interference cancellation concurrently for overlapped multiple access. In power-domain NOMA systems, users who have distinct channels conditions can achieve higher performance gain than the users who have similar channel conditions [6], [7]. To facilitate the implementation of NOMA, RIS/STAR-RIS is an ideal candidate for intelligent NOMA by alternating the propagation environments for the needs of NOMA [8]. Specifically, the direction of a user's channel vector can be effectively and intelligently tuned and the communication area can be expanded by applying STAR-RIS in NOMA. Moreover, the application of multiple-input multiple-output (MIMO) technology can provide additional degrees of freedom to the signal propagation. In this paper, we focus on the STAR-RIS enabled MIMO-NOMA system and exploit its full potential on the system energy efficiency improvement, which has not been well studied in the existing research works.

A. Related Literature

With the growing research attention of RIS, several related areas including RIS aided NOMA, STAR-RIS and STAR-RIS aided NOMA, have been extensively studied in the literature.

Manuscript received 24 May 2022; revised 20 September 2022; accepted 9 November 2022. Date of publication 21 November 2022; date of current version 16 January 2023. The work of Shu Fu was supported by the National Natural Science Foundation of China under Grant 62271093 and Grant U21A20448. The work of Zhiguo Ding was supported by the UK EPSRC under grant number EP/ W034522/1, by H2020 H2020-MSCA-RISE-2020 under grant number 101006411. The associate editor coordinating the review of this article and approving it for publication was L. Song. *(Corresponding author: Shu Fu.)*

Fang Fang is with the Department of Electrical and Computer Engineering and the Department of Computer Science, Western University, London, ON N6A 3K7, Canada (e-mail: fang.fang@uwo.ca).

Bibo Wu and Shu Fu are with the College of Microelectronics and Communication Engineering, Chongqing University, Chongqing 400044, China (e-mail: bibowu@cqu.edu.cn; shufu@cqu.edu.cn).

Zhiguo Ding is with the School of Electrical and Electronic Engineering, The University of Manchester, M13 9PL Manchester, U.K. (e-mail: zhiguo.ding@manchester.ac.uk).

Xianbin Wang is with the Department of Electrical and Computer Engineering, Western University, London, ON N6A 3K7, Canada (e-mail: xianbin.wang@uwo.ca).

Color versions of one or more figures in this article are available at https://doi.org/10.1109/TCOMM.2022.3223706.

Digital Object Identifier 10.1109/TCOMM.2022.3223706

1) RIS aided NOMA systems: Driven by the advantages of RIS-NOMA systems, such as an excess of degrees of freedom in the spatial, frequency, and time domains [8], resource allocation/optimization has attracted extensive research attention to further improve the communication performance. The strength of the received signal can be significantly improved by jointly optimizing the communication resource, e.g., beamforming, power and subchannel, and the reflection angles and amplitude coefficients of each element on RISs. Various optimization problems and solutions have been investigated in existing research, including power minimization [9], [10], [11], sum rate maximization [12], [13], [14], [15], and energy efficiency maximization [16], [17]. The traditional resource optimization methods, such as convex optimization, matching theory, and game theory, have been well studied in NOMA networks [18] and RIS communication systems [13]. To support ultra-fast communication, the resource allocation, including user grouping/clustering, subchannel assignment, the beamforming design, power allocation and phase shift optimizaton must embrace intelligence to adapt the fast time-varying wireless environment. To reduce the complexity of the traditional convex optimization approaches, such as semidefinte relaxation (SDR) and successive convex approximation (SCA) [16], deep learning (DL) and reinforcement learning (RL) techniques, such as deep Q-networks (DQN), have been utilized to provide smart control for the RIS with NOMA transmission. In [19], a K-means based method and DQN based algorithm were proposed for user clustering and a joint design of phase shift matrix and power allocation, respectively. However, DQN can only handle discrete actions, such as quantified phase shifts. As one of sophisticated deep reinforcement learning methods, deep deterministic policy gradient (DDPG) combines DQN and the policy gradient algorithm, and can be applicable to the DQN problem with the continuous actions, such as continuous power allocation. Thus, the phase shift of the RIS can be designed by DDPG to maximize the system sum rate in RIS-NOMA [20], [21]. Moreover, RIS-NOMA has high flexibility to combine with other key technologies in 6G, e.g., millimeter wave (mmWave) [22], [23], MIMO [24], and unmanned aerial vehicle (UAV) communications [25], etc.
2) STAR-RIS systems: Recently, STAR-RIS has emerged to provide larger communication coverage compared to reflecting-only RIS [5]. Intelligent omni-surface (IOS)-assisted communication was studied to maximize the spectral efficiency by the proposed branch-and-bound based phase shift optimization algorithm [26]. The authors in [27] proposed an IOS aided indoor communication system and designed a distributed hybrid beamforming scheme consisting of digital beamforming at access points (APs) and IOS-based analog beamforming to maximize the sum rate. Three practical operating protocols, namely energy splitting, mode switching, and time switching, were proposed for STAR-RIS [28]. In this work, both unicast and multicast transmission were considered to minimize the system power minimization by the proposed joint active and passive beamforming optimization scheme.
3) STAR-RIS aided NOMA systems: There are still handful research works investigating STAR-RIS aided NOMA networks. Compared to STAR-RIS-orthogonal multiple access (OMA) scheme, STAR-RIS-NOMA can achieve higher system sum rate by optimizing subchannels, decoding orders, beamforming-coefficient vectors, and power allocation [29]. Considering the decoding order of the NOMA users, the authors in [30] investigated the sum rate maximization by optimizing power allocation, active and passive beamforming in STAR-RIS systems. In order to adapt the time-varying wireless environment, machine learning techniques can be used for the intelligent control for RIS-NOMA systems. In [31], the system energy efficiency maximization problem was investigated for a STAR-RIS aided NOMA downlink network. In this work, a DDPG-based algorithm was proposed to jointly optimize the transmission beamforming vectors at the base station and the coefficients matrices at the STAR-RIS aiming to maximize the system energy efficiency.

B. Motivations and Contributions

Driven by the advantages of STAR-RIS in wireless communications, e.g., large communication coverage and tunable wireless channels, applying STAR-RIS in NOMA can further improve the communication performance in terms of further enhanced data rate and spectral efficiency. In order to provide the flexibility and spatial degrees of freedom to the signal propagation, MIMO has been widely used in B5G and 6G. It has been proved that the coexistence of NOMA and MIMO outperforms conventional MIMO-OMA scheme [32], [33]. Motivated by this, in this paper, we mainly focus on the STAR-RIS enabled MIMO-NOMA network. One goal of our study is to exploit the full potential of STAR-RIS enabled MIMO-NOMA network via joint optimization of the active beamforming/resource allocation at the BS, and the transmission and reflection coefficients at the STAR-RIS, which is challenging to optimize due to the highly coupled optimization variables. Differing from existing works on STAR-RISs enabled NOMA networks [29], [30], [31] which did not consider MIMO technology, this work focuses on developing novel energy-efficient resource allocation strategy for the STAR-RIS enabled MIMO-NOMA communication network, where the joint optimization of beamforming vectors and the STAR-RIS element matrix are involved. More specifically, due to the complexity of MIMO system, we propose a novel mechanism which combines signal alignment and zero-forcing precoding methods to decompose MIMO-NOMA channels into single-antenna NOMA channels, thus de-complicating the system. In order to obtain the optimal power allocation, we utilize the Dinkelbach approach to transform the original fractional objective function into a more tractable nonfractional form. And SCA is utilized in the phase shift optimization subproblem. The proposed energy-efficient resource allocation scheme can provide an effective solution to maximize the system energy efficiency. The main contributions are summarized as follows.

1) We consider a downlink STAR-RIS assisted MIMO-NOMA communication network, where one STAR-RIS is deployed to assist the communication from the BS to the clustered users with multiple antennas. We consider two types of user pairs in the system, which are distributed in the transmission and reflection zones of the STAR-RIS, respectively. We formulate the system energy efficiency maximization problem by jointly optimizing the power allocation coefficients, active beamforming at the BS and the phase shift variables at the STAR-RIS. The formulated problem is non-convex and challenging to solve due to highly coupled optimization variables. To efficiently address this tacking problem, we divide the original problem into two sub-problems, i.e., beamforming optimization and phase shift optimization, and then solve them alternatively.
2) For beamforming design, we propose a novel scheme which consists of precoding design and power allocation. Specifically, we initially utilize signal alignment and zero-forcing methods to decompose MIMO-NOMA channels into single-antenna NOMA channels, which simplifies the later analysis significantly. Subsequently, a zero-forcing based precoding matrix can be designed effectively. Based on the simplified system, we transform the original fractional optimization problem into a more tractable nonfractional form by introducing auxiliary variables based on the proposed Dinkelbach approach, which is guaranteed to converge. Then, the optimal solution is obtained through dual decomposition as well as the Karush-Kuhn-Tucker (KKT) conditions.
3) Given by the obtained beamforming strategy, the original energy efficiency maximization problem can be transformed into a sum rate maximization problem, which is also non-convex and challenging to solve. In order to tackle the phase shift optimization problem, We propose an SCA based scheme, where a series of auxiliary variables are introduced and the subsequent convex objective function is formed. Under this circumstance, the derived objective optimization problem is convex and can be solved effectively through convex optimization tools, such as CVX.

C. Organization

The rest of this paper is organized as follows. In Section II, we introduce the downlink STAR-RIS assisted MIMO-NOMA system model and formulate the energy efficiency maximization problem. In Section III, we decompose the original objective problem into two sub-problems, including beamforming optimization and phase shift optimization, and propose an iterative algorithm to solve them. Numerical results are presented in Section IV, which is followed by the conclusion in Section V.

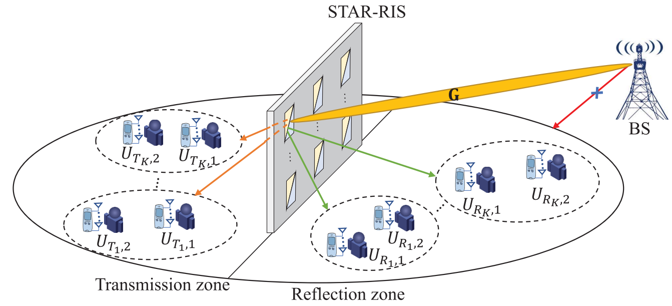

Fig. 1. A STAR-RIS assisted MIMO-NOMA network.

II. System Model and Problem Formulation

A. STAR-RIS Assisted MIMO-NOMA System

As shown in Fig. 1, we consider a STAR-RIS assisted downlink MIMO-NOMA communication network, where a BS communicates with multiple user groups with the aid of a STAR-RIS consisting of M elements. In this system, the BS and users are equipped with multiple antennas, and the number of antennas for both the BS and all users is N. As illustrated in Fig. 1, for simplicity, in this paper we make such an assumption that all the user pairs are formed in advanced based on the location of users [34], [35]. We define the users located behind the STAR-RIS (namely, transmission region) as T user pairs, while the user pairs located in front of the STAR-RIS (namely, reflection region) are referred to as R user pairs. We assume that the number of T user pairs is equal to the number of R, which is set to K. Note we defined the number of T user pairs and R user pairs to be equal based on the characteristic of the STAR-RIS. Each element of the STAR-RIS can transmit and reflect the incident signal simultaneously, thus generating the same number of the transmitting beams and the reflecting beams. Under this circumstance, we assume that the number of T user pairs and R user pairs is equal in order to guarantee all users in our system can be served at the same time. We define the j-th user in the k-th user pair as $U_{k,j}$, where $j \in \{1, 2\}$ is the index of users in each user pair, and $k \in \mathcal{K} = \{\mathrm{T}_1, \mathrm{T}_2, \ldots, \mathrm{T}_K, \mathrm{R}_1, \mathrm{R}_2, \ldots, \mathrm{R}_K\}$ is the index of user pairs in both transmission and reflection zones. In this paper, we assume that the direct communication links between the BS and the two kinds of users are blocked by the block buildings. In this system model, the messages intended to be received by $U_{k,1}$, $U_{k,2}$ are defined as $s_{k,1}$, $s_{k,2}$, respectively, and $\mathbf{w}_k \in \mathbb{C}^{N\times 1}$ is the linear precoding vector for the k-th user pair. In this STAR-RIS-assisted MIMO-NOMA system, we consider that the BS assigns different power levels to the signals being sent to the users in one pair. The BS broadcasts the superposition signal, which can be expressed as

$$\mathbf{s} = \sum_{k\in\mathcal{K}} \mathbf{w}_k \left(\sqrt{p_{k,1}} s_{k,1} + \sqrt{p_{k,2}} s_{k,2}\right), \tag{1}$$

where $p_{k,1}$ and $p_{k,2}$ represent the transmit power of $U_{k,1}$ and $U_{k,2}$, respectively.

In this paper, we assume perfect channel state information (CSI) is available. In this case, the STAR-RIS is able to properly adjust the phase shift under the aid of a smart controller and the BS can generate the proper beams. Assuming non-dispersive narrow-band transmission, the baseband equivalent channels spanning from the BS to the STAR-RIS and from the STAR-RIS to $U_{k,j}$ are modelled by the matrices $\mathbf{G} \in \mathbb{C}^{M\times N}$ and $\mathbf{h}_{k,j} \in \mathbb{C}^{M\times N}$, respectively. We can model $\mathbf{G}$ as the following Rician fading channel:

$$\mathbf{G} = \sqrt{\frac{\rho_0}{d^{\alpha_{BR}}}} \left(\sqrt{\frac{K_{BR}}{K_{BR}+1}} \mathbf{G}^{\mathrm{LoS}} + \sqrt{\frac{1}{K_{BR}+1}} \mathbf{G}^{\mathrm{NLoS}} \right), \tag{2}$$

where $\mathbf{G}^{\mathrm{LoS}}$ and $\mathbf{G}^{\mathrm{NLoS}}$ are the deterministic line-of-sight (LoS) component and the random non-line-of-sight (NLoS) component modeled as Rayleigh fading, respectively. d denotes the distance between BS and STAR-RIS. $\alpha_{BR} \geq 2$ denotes the path loss exponent, ρ_0 represents the path loss at a reference distance of 1 meter. K_{BR} denotes the Rician factor. For simplicity, we use $\bar{\mathbf{G}}$ to represent the summed terms of $\mathbf{G}^{\mathrm{LoS}}$ and $\mathbf{G}^{\mathrm{NLoS}}$, i.e., $\bar{\mathbf{G}} = \sqrt{\frac{K_{BR}}{K_{BR}+1}}\mathbf{G}^{\mathrm{LoS}} + \sqrt{\frac{1}{K_{BR}+1}}\mathbf{G}^{\mathrm{NLoS}}$. Similarly, the Rician fading channel from the STAR-RIS to $U_{k,j}$ is expressed as:

$$\mathbf{h}_{k,j} = \sqrt{\frac{\rho_0}{D_{k,j}^{\alpha_{RU}}}} \left(\sqrt{\frac{K_{RU}}{K_{RU}+1}} \mathbf{h}_{k,j}^{\mathrm{LoS}} + \sqrt{\frac{1}{K_{RU}+1}} \mathbf{h}_{k,j}^{\mathrm{NLoS}} \right), \tag{3}$$

where $\mathbf{h}_{k,j}^{\mathrm{LoS}}$ and $\mathbf{h}_{k,j}^{\mathrm{NLoS}}$ are the LoS and NLoS components, respectively, and $D_{k,j}$ denotes the distance between the STAR-RIS and $U_{k,j}$. α_{RU} and K_{RU} are path loss exponent and Rician factor, respctively. For simplicity, we use $\bar{\mathbf{h}}_{k,j}$ to represent the summed terms of $\mathbf{h}_{k,j}^{\mathrm{LoS}}$ and $\mathbf{h}_{k,j}^{\mathrm{NLoS}}$.

In order to reduce the overhead for information exchange between the BS and the STAR-RIS, we assume that all elements have the same amplitude coefficients. Let $\mathbf{\Theta}_n = \sqrt{\beta_n}\mathrm{diag}\left(\mathrm{e}^{\mathrm{j}\theta_1^n}, \ldots, \mathrm{e}^{\mathrm{j}\theta_M^n}\right)$ denote the STAR-RIS coefficient matrix, and $n \in \{\mathrm{T}, \mathrm{R}\}$. Specifically, for T users, i.e., $k \in \{\mathrm{T}_1, \mathrm{T}_2, \ldots, \mathrm{T}_K\}$, $n = \mathrm{T}$; for R users, i.e., $k \in \{\mathrm{R}_1, \mathrm{R}_2, \ldots, \mathrm{R}_K\}$, $n = \mathrm{R}$. In this case, $\mathbf{\Theta}_{\mathrm{T}}$ denotes the transmission-coefficient matrix, and $\mathbf{\Theta}_{\mathrm{R}}$ denotes the reflection-coefficient matrix of the STAR-RIS. Moreover, $\sqrt{\beta_n} \in [0, 1]$ which is set to a constant and $\theta_m^n \in [0, 2\pi)$, $m \in \{1, \ldots, M\}$ characterize the amplitude and phase shift adjustments imposed on the incident signals facilitated by the m-th element. Note that due to the law of energy conservation, the sum energy of the transmitted and reflected signals has to be equal to that of the incident signals. Thus, we have $\beta_{\mathrm{T}} + \beta_{\mathrm{R}} = 1$. The received signals at $U_{k,j}$ is

$$\mathbf{y}_{k,j} = \Delta_{k,j}\mathbf{Z}_{k,j} \sum_{k\in\mathcal{K}} \mathbf{w}_k \left(\sqrt{p_{k,1}} s_{k,1} + \sqrt{p_{k,2}} s_{k,2} \right) + \mathbf{n}_{k,j}, \tag{4}$$

where $\Delta_{k,j} = \frac{\rho_0}{\sqrt{d^{\alpha_{BR}} D_{k,j}^{\alpha_{RU}}}}$ and $\mathbf{Z}_{k,j} = \bar{\mathbf{h}}_{k,j}^H \mathbf{\Theta}_n \bar{\mathbf{G}}$ which denotes the equivalent channel spanning from the BS to $U_{k,j}$ and $\mathbf{n}_{k,j}$ is the noise vector satisfying $\mathcal{CN}\left(0, \sigma^2\right)$.

To improve the spectrum efficiency, NOMA is applied between the two users in each pair, which is a basic case studied in previous works considering the complexity of successive interference cancellation (SIC). In the downlink RIS-assisted NOMA systems, the performance of SIC is highly affected to the decoding order, which indicates that when decoding one user's signal, the interference from the users whose signals have been decoded before could be cancelled. According to the principle of NOMA in downlink communications, higher powers are allocated to the users with lower channel gains [34]. Hence, in a NOMA system, one user is able to decode signals of users with higher powers and remove them from its own signal, but treats the signals from other user with lower powers as interference. In single-antenna NOMA systems, the optimal signal decoding order is the same as the ascending order of the channel gains. However, this decoding order method cannot be used directly in RIS enhanced MIMO-NOMA systems. This is because the end-to-end channels can be modified by the RIS. It is worthy pointing out that, in this paper, our focus is to investigate the energy efficient potential of STAR-RIS in the MIMO-NOMA system instead of to design optimal decoding order in NOMA. Note in our proposed STAR-RIS aided NOMA system, the difference between the equivalent channel gains of the two users in a pair is inevitable, i.e., there always exist the user with stronger equivalent channel gain and the other with weaker equivalent channel gain. Thus, without loss of generality and in order to reduce the complexity of the design, we assume the decoding order as $(U_{k,2}, U_{k,1})$ in the k user pair. In this case, $U_{k,1}$ first decodes the signal of $U_{k,2}$ and subtracts this from its received signal, which means $U_{k,1}$ can decode its signal without interference. For $U_{k,2}$, it does not perform SIC and simply decodes its signal by treating $U_{k,1}$'s signal as interference. Therefore, the achievable rate of these two users are respectively given by [36]

$$R_{k,1} = \log_2 \left(1 + \frac{\left|\Delta_{k,1}\mathbf{Z}_{k,1}\mathbf{w}_k\right|^2 p_{k,1}}{\sum\limits_{i\in\mathcal{K}} \sum\limits_{j=1}^{2} \left|\Delta_{k,1}\mathbf{Z}_{k,1}\mathbf{w}_i\right|^2 p_{i,j} + \sigma^2} \right), \tag{5}$$

$$R_{k,2} = \min\left\{ \log_2\left(1 + SINR_{2,1}^k\right), \log_2\left(1 + SINR_{2,2}^k\right) \right\}, \tag{6}$$

where $\sum\limits_{i\in\mathcal{K}} \sum\limits_{j=1}^{2} \left|\Delta_{k,1}\mathbf{Z}_{k,1}\mathbf{w}_i\right|^2 p_{i,j}$ denotes the inter-pair interference and we have $i \neq k$. Besides, we have

$$SINR_{2,1}^k = \frac{\left|\Delta_{k,1}\mathbf{Z}_{k,1}\mathbf{w}_k\right|^2 p_{k,2}}{\left|\Delta_{k,1}\mathbf{Z}_{k,1}\mathbf{w}_k\right|^2 p_{k,1} + \sum\limits_{i\in\mathcal{K}} \sum\limits_{j=1}^{2} \left|\Delta_{k,1}\mathbf{Z}_{k,1}\mathbf{w}_i\right|^2 p_{i,j} + \sigma^2}, \tag{7}$$

$$SINR_{2,2}^k = \frac{\left|\Delta_{k,2}\mathbf{Z}_{k,2}\mathbf{w}_k\right|^2 p_{k,2}}{\left|\Delta_{k,2}\mathbf{Z}_{k,2}\mathbf{w}_k\right|^2 p_{k,1} + \sum\limits_{i\in\mathcal{K}} \sum\limits_{j=1}^{2} \left|\Delta_{k,2}\mathbf{Z}_{k,2}\mathbf{w}_i\right|^2 p_{i,j} + \sigma^2}, \tag{8}$$

where $\left|\Delta_{k,1}\mathbf{Z}_{k,1}\mathbf{w}_k\right|^2 p_{k,1}$ and $\left|\Delta_{k,2}\mathbf{Z}_{k,2}\mathbf{w}_k\right|^2 p_{k,1}$ indicate the intra-pair interference, and $SINR_{2,1}^k$ and $SINR_{2,2}^k$ respectively denote the signal interference noise ratio (SINR) of $U_{k,2}$

decoded at $U_{k,1}$ and the SINR of $U_{k,2}$ decoded at itself. The reason why there exists the min constraint is to ensure the successful utilization of SIC at $U_{k,1}$. In fact, the achievable rate of $U_{k,2}$ decoded at $U_{k,1}$ reflects the threshold of decoding the signal of $U_{k,2}$ at $U_{k,1}$. Thus, if the achievable rate of $U_{k,2}$ is larger than the decoding threshold at $U_{k,1}$, $U_{k,1}$ cannot decode the signal of $U_{k,2}$ successfully, leading to the failure of SIC. In this case, it is impossible for $U_{k,1}$ to decode its own signal by moving the decoded signal of $U_{k,2}$. Thus, the min limit in $R_{k,2}$ guarantees the success of performing SIC at $U_{k,1}$.

B. Problem Formulation

In this STAR-RIS assisted MIMO-NOMA system, we aim to maximize the system energy efficiency, which is defined as a ratio of the system sum rate and the total power consumption. Let us denote the total circuit power at the BS by P_c which is regarded as a static power consumption. Note that we ignore the circuit power consumption related to the elements of the STAR-RIS in this paper, and only consider that related to the controller, which can be regarded as a constant. In fact, due to the property of low cost, it is reasonable to make such a consumption which can be seen in many works regarding RIS, such as in [37] and [38]. We also set a parameter $\eta \in [0,1]$ to denote the power amplifier coefficient at the BS. Considering the individual data rate constraints and the total transmit power budget, the energy efficiency maximization problem can be formulated as

$$\max_{\mathbf{\Theta}_n,\mathbf{w}_k,p_{k,j}} \frac{\sum\limits_{k\in\mathcal{K}} (R_{k,1}+R_{k,2})}{\frac{1}{\eta}\sum\limits_{k\in\mathcal{K}} (p_{k,1}+p_{k,2})+P_c} \tag{9a}$$

$$\text{s.t.} \quad R_{k,j} \geq R_{k,j}^{\min}, j=1,2, \tag{9b}$$

$$\sum_{k\in\mathcal{K}} (p_{k,1}+p_{k,2}) \leq P_{\max}, \tag{9c}$$

$$0 \leq \theta_m^n < 2\pi, m=1,\ldots,M, \tag{9d}$$

where $R_{k,j}^{\min}$ denotes the minimum data rate requirements for $U_{k,j}$ and $R_{k,j}^{\min}=\log_2\left(1+\Gamma_{k,j}^{\min}\right)$, and where $\Gamma_{k,j}^{\min}=2^{R_{k,j}^{\min}}-1$ is the minimum SINR for $U_{k,j}$, which is a known parameter. Constraint (9b) guarantees the QoS requirement for $U_{k,j}$. Constraint (9c) limits the total transmit power to $P_{\max}$. Constraint (9d) specifies the range of phase shift. However, $R_{k,j}$ is not jointly concave with respect to $\mathbf{\Theta}_n$, $\mathbf{w}_k$ and $p_{k,j}$. It is challenging to obtain the globally optimal solution to problem (9) due to its non-convexity.

III. Alternating Optimization Solution

The original formulated problem (9) is a fractional form and non-convex. Thus, in this section, an alternating optimization-based algorithm is proposed to solve problem (9) efficiently. Specifically, we decouple problem (9) into beamforming optimization and phase shift optimization subproblems, and then solve these two subproblems alternatively. The beamforming optimization includes precoding matrix design and power allocation. In particular, given the fixed $\mathbf{\Theta}_n$, we first decompose the multi-user MIMO-NOMA channels into single-antenna NOMA channels with the use of zero-forcing precoding method. Then, the Dinkelbach approach and dual decomposition are exploited to optimize the power allocation. Subsequently, based on the optimized precoding matrix and power allocation, the sequential convex approximation and SCA are exploited to optimize $\mathbf{\Theta}_n$. We solve these two subproblems alternatively until the convergence, and then the original objective problem (9) is solved efficiently. It is worth noting that even though the alternating algorithm is widely used in the existing works [2], [16], the proposed solutions to beamforming optimization and phase optimization in this paper are different from the existing algorithms. Specifically, in the proposed algorithm, we utilize the zero-forcing precoding method to decompose the multi-user MIMO-NOMA channels into single-antenna NOMA channels, and propose the Dinkelbach-based and SCA-based schemes to address the beamforming optimization and phase shift optimization, respectively.

A. Beamforming Optimization

For given phase shift $\mathbf{\Theta}_n$, problem (9) is still non-convex. In order to reduce to the complexity of the system, we use zero-forcing precoding method to eliminate the inter-pair interference and achieve the decomposition of the MIMO channels. In the zero-forcing precoding strategy, the users transmit data in the null space of other users' channels, which effectively mitigates the inter-pair interference. In the proposed system model, if the channels of the different user pairs are orthogonal, the inter-pair interference can be avoided by using zero-forcing precoding method. Thus, we can achieve the best performance in our system if the channels of users in different pairs are orthogonal. Specifically, $U_{k,j}$ applies detection vectors $\mathbf{v}_{k,j} \in \mathbb{C}^{N\times 1}$ to its received signal, and therefore the received signal of $U_{k,j}$ can be rewritten as

$$\begin{aligned}\mathbf{v}_{k,j}^H\mathbf{y}_{k,j} &= \Delta_{k,j}\mathbf{v}_{k,j}^H\mathbf{Z}_{k,j}\sum\nolimits_{k\in\mathcal{K}}\mathbf{w}_k\left(\sqrt{p_{k,1}}s_{k,1}+\sqrt{p_{k,2}}s_{k,2}\right)\\ &\quad+\mathbf{v}_{k,j}^H\mathbf{n}_{k,j}\\ &= \Delta_{k,j}\mathbf{v}_{k,j}^H\mathbf{Z}_{k,j}\mathbf{w}_k\left(\sqrt{p_{k,1}}s_{k,1}+\sqrt{p_{k,2}}s_{k,2}\right)\\ &\quad+\Delta_{k,j}\mathbf{v}_{k,j}^H\mathbf{Z}_{k,j}\sum\nolimits_{i\neq k}\mathbf{w}_i\left(\sqrt{p_{i,1}}s_{i,1}+\sqrt{p_{i,2}}s_{i,2}\right)\\ &\quad+\mathbf{v}_{k,j}^H\mathbf{n}_{k,j}.\end{aligned} \tag{10}$$

In this paper, the concept of signal alignment is applied in the k user pair. Note that signal alignment can be viewed as a special case of interference alignment which can effectively exploit the excess degrees of freedom in MIMO systems for suppressing co-channel interference [35]. Thus, the detection vectors are designed to satisfy the following constraint:

$$\mathbf{v}_{k,1}^H\mathbf{Z}_{k,1}=\mathbf{v}_{k,2}^H\mathbf{Z}_{k,2}, \tag{11}$$

or equivalently $\begin{bmatrix}\mathbf{Z}_{k,1}^H & -\mathbf{Z}_{k,2}^H\end{bmatrix}\begin{bmatrix}\mathbf{v}_{k,1}\\ \mathbf{v}_{k,2}\end{bmatrix}=\mathbf{0}_{N\times 1}$. Note that $\begin{bmatrix}\mathbf{Z}_{k,1}^H & -\mathbf{Z}_{k,2}^H\end{bmatrix}$ is a $N\times 2N$ matrix, so such $\mathbf{v}_{k,1}$ and $\mathbf{v}_{k,2}$ always exist. Denote $\mathbf{x}_k$ as one normalized vector from the null space of $\begin{bmatrix}\mathbf{Z}_{k,1}^H & -\mathbf{Z}_{k,2}^H\end{bmatrix}$. So $\mathbf{v}_{k,1}=\sqrt{2N}\mathbf{I}_1\mathbf{x}_k$ and $\mathbf{v}_{k,2}=\sqrt{2N}\mathbf{I}_2\mathbf{x}_k$ where $\mathbf{I}_1=[\mathbf{I}_N \;\; \mathbf{0}_{N,N}]$, $\mathbf{I}_2=[\mathbf{0}_{N,N} \;\; \mathbf{I}_N]$, $\mathbf{I}_N$ is a

$N\times N$ identity matrix and $\mathbf{0}_{N,N}$ is a $N\times N$ zero matrix. The reason to have the factor $\sqrt{2N}$ in the expression of $\mathbf{v}_{k,j}$ is to ensure that the instantaneous total transmission power for each pair is always constrained as $p_{k,1}|\mathbf{v}_{k,1}|^2+p_{k,2}|\mathbf{v}_{k,2}|^2=2N$.

The effect of the signal alignment based designed in (11) is the projection of the channels of the two users in the same pair into the same direction. Define $\mathbf{g}_k \triangleq \mathbf{Z}_{k,1}^H\mathbf{v}_{k,1}$ as the effective channel vector shared by $U_{k,1}$ and $U_{k,2}$ in the k user pair. In order to remove the inter-pair interference, a zero-forcing precoding method is utilized. Specifically, for the k user pair, we design its beamforming vector $\mathbf{w}_k$ to satisfy the orthogonality with the effective channel vectors of other user pairs. Thus, the following constraint has to be met:

$$\mathbf{g}_i^H\mathbf{w}_k=0,\ i\neq k, \tag{12}$$

which achieves channel orthogonality between different pairs. Thus, a zero-forcing based precoding matrix can be designed as [35]

$$\mathbf{w}_k=\mathbf{E}^{-H}\mathbf{D}, \tag{13}$$

where $\mathbf{E} \triangleq [\mathbf{g}_{\mathrm{T}_1},\cdots\mathbf{g}_{\mathrm{T_K}},\mathbf{g}_{\mathrm{R}_1},\cdots\mathbf{g}_{\mathrm{R_K}}]^H \triangleq [\mathbf{g}_1,\cdots\mathbf{g}_K,\mathbf{g}_{K+1},\cdots\mathbf{g}_{2K}]^H$ which is a $2K\times N$ matrix denotes the set of effective channel vectors of all user pairs. Note here we establish a correspondence between the k user pair and the index in $\mathbf{E}$. And $\mathbf{D}$ is a diagonal matrix to ensure beamforming normalization at the BS, i.e., $\mathbf{D}^2=\mathrm{diag}\left\{\frac{1}{(\mathbf{E}^{-1}\mathbf{E}^{-\mathrm{H}})_{1,1}}\cdots\frac{1}{(\mathbf{E}^{-1}\mathbf{E}^{-\mathrm{H}})_{2\mathrm{K},2\mathrm{K}}}\right\}$, where $(\mathbf{A})_{m,m}$ denotes the m-th elements on the main diagonal of $\mathbf{A}$. Given this zero-forcing precoding design, the received signals of $U_{k,j}$ can be decoupled as

$$y_{k,j}=h_{k,j}\left(\sqrt{p_{k,1}}s_{k,1}+\sqrt{p_{k,2}}s_{k,2}\right)+n_{k,j}, \tag{14}$$

where $y_{k,j}=\mathbf{v}_{k,j}^H\mathbf{y}_{k,j}$, $h_{k,j}=\Delta_{k,j}\mathbf{g}_k\mathbf{w}_k$ and $n_{k,j}=\mathbf{v}_{k,j}^H\mathbf{n}_{k,j}\sim\mathcal{CN}\left(0,\sigma^2\right)$. Therefore, the use of the signal alignment, zero-forcing based precoding and detection matrices decomposes the multi-user STAR-RIS assisted MIMO-NOMA channels into $2K$ single-antenna NOMA channels. Remember in this paper, we set the equivalent channel gain of $U_{k,2}$ is small than that of $U_{k,1}$ in the k user pair. Referring to the similar analysis in the last section, we can obtain the achievable rate of $U_{k,1}$ and $U_{k,2}$ in such a single-antenna NOMA system. According to the principle of NOMA in downlink communications, higher powers are allocated to the users with lower channel gains [34], thus opportunistically allocating the transmit power to different users, from which we have $p_{k,1}\le p_{k,2}$. Moreover, the users with better channel conditions will utilize SIC strategy, i.e., they first decode the signals of the users with poorer channel conditions and then decode their own by removing the other users' signals, leading to the decoding order as $(U_{k,2},U_{k,1})$ in the k user pair in our proposed system. Therefore, there exists the min limit in the expression of the achievable rate of $U_{k,2}$ in order to perform SIC at $U_{k,1}$ successfully. Nevertheless, after applying the zero-forcing precoding method, the inter-pair interference in the system is cancelled. Under this circumstance, we can easily proof that the SINR of $U_{k,2}$ decoded at itself is always smaller than that decoded at $U_{k,1}$. Thus, we can ignore the min limit in the expression of the achievable rate of $U_{k,2}$. Thus, the achievable rate of $U_{k,1}$ and $U_{k,2}$ can now be respectively rewritten as

$$R'_{k,1}=\log_2\left(1+\frac{|h_{k,1}|^2p_{k,1}}{\sigma^2}\right), \tag{15}$$

$$R'_{k,2}=\log_2\left(1+\frac{|h_{k,2}|^2p_{k,2}}{|h_{k,2}|^2p_{k,1}+\sigma^2}\right). \tag{16}$$

Given the fixed phase shift $\mathbf{\Theta}_n$ and the designed precoding matrix $\mathbf{w}_k$, the original problem (9) can be transformed to the following problem:

$$\max_{p_{k,1},p_{k,2}} \frac{\sum\limits_{k\in\mathcal{K}}\left(R'_{k,1}+R'_{k,2}\right)}{\frac{1}{\eta}\sum\limits_{k\in\mathcal{K}}(p_{k,1}+p_{k,2})+P_c} \tag{17a}$$

$$\mathrm{s.t.}\quad R'_{k,j}\ge R_{k,j}^{\min} j=1,2, \tag{17b}$$

$$0\le p_{k,1}\le p_{k,2}, \tag{17c}$$

$$\sum_{k\in\mathcal{K}}(p_{k,1}+p_{k,2})\le P_{\max}. \tag{17d}$$

Problem (17) is a non-convex and fractional optimization problem. To solve (17), we first introduce auxiliary variables $\mathbf{q}=\{q_k\}_{k\in\mathcal{K}}$ that represent the power budgets in each user pair k with $p_{k,1}+p_{k,2}=q_k$ [39]. Then, (17) is decomposed into a group of subproblems for each channel k:

$$\max_{p_{k,1},p_{k,2}} \frac{R'_{k,1}+R'_{k,2}}{\frac{1}{\eta}\sum\limits_{k\in\mathcal{K}}q_k+P_c} \tag{18a}$$

$$\mathrm{s.t.}\quad R'_{k,1}\ge R_{k,1}^{\min}, \tag{18b}$$

$$R'_{k,2}\ge R_{k,2}^{\min}, \tag{18c}$$

$$0\le p_{k,1}\le p_{k,2}, \tag{18d}$$

$$p_{k,1}+p_{k,2}=q_k. \tag{18e}$$

Since $p_{k,2}=q_k-p_{k,1}$, $R'_{k,1}+R'_{k,2}$ can be rewritten as

$$T\left(p_{k,1}\right)=\log_2\left(1+\frac{|h_{k,1}|^2p_{k,1}}{\sigma^2}\right) +\log_2\left(\frac{|h_{k,2}|^2q_k+\sigma^2}{|h_{k,2}|^2p_{k,1}+\sigma^2}\right) \tag{19}$$

We take the derivative of $T\left(p_{k,1}\right)$ and have

$$\frac{dT\left(p_{k,1}\right)}{dp_{k,1}}=\frac{|h_{k,1}|^2}{\ln 2\left(|h_{k,1}|^2p_{k,1}+\sigma^2\right)} -\frac{|h_{k,2}|^2}{\ln 2\left(|h_{k,2}|^2p_{k,1}+\sigma^2\right)} \tag{20}$$

Due to $h_{k,1}\ge h_{k,2}$, we have $\frac{dT(p_{k,1})}{dp_{k,1}}\ge 0$, which implies that $T\left(p_{k,1}\right)$ is monotonically nondecreasing, so the maximum is achieved at the upper bound of $p_{k,1}$. From $R'_{k,1}\ge R_{k,1}^{\min}$ and $R'_{k,2}\ge R_{k,2}^{\min}$, we obtain

$$\frac{\left(2^{R_{k,1}^{\min}}-1\right)\sigma^2}{|h_{k,1}|^2}\le p_{k,1}\le\frac{|h_{k,2}|^2q_k+\sigma^2}{2^{R_{k,2}^{\min}}|h_{k,2}|^2}-\frac{\sigma^2}{|h_{k,2}|^2}, \tag{21}$$

which holds if and only if $\frac{\left(2^{R_{k,1}^{\min}}-1\right)\sigma^2}{|h_{k,1}|^2} \le \frac{|h_{k,2}|^2 q_k+\sigma^2}{2^{R_{k,2}^{\min}}|h_{k,2}|^2} - \frac{\sigma^2}{|h_{k,2}|^2}$, i.e., $q_k \ge \Upsilon_k$, where

$$\Upsilon_k = \left(\frac{\left(2^{R_{k,1}^{\min}}-1\right)\sigma^2}{\left|h_{k,1}\right|^2} + \frac{\sigma^2}{\left|h_{k,2}\right|^2}\right)2^{R_{k,2}^{\min}} - \frac{\sigma^2}{\left|h_{k,2}\right|^2}. \quad (22)$$

Thus, the optimal solution is

$$p_{k,1}^* = \frac{\left|h_{k,2}\right|^2 q_k+\sigma^2}{2^{R_{k,2}^{\min}}\left|h_{k,2}\right|^2} - \frac{\sigma^2}{\left|h_{k,2}\right|^2}, \quad p_{k,2}^* = q_k - p_{k,1}^*. \quad (23)$$

In the following, we focus on optimizing the channel power budget q_k for each user pair. According to (23), the power budget optimization problem is given by

$$\max_{\mathbf{q}} \ \frac{\sum\limits_{k\in\mathcal{K}}\left(R_{k,1}^* + R_{k,2}^*\right)}{\frac{1}{\eta}\sum\limits_{k\in\mathcal{K}} q_k + P_c} \quad (24a)$$

$$\text{s.t.} \quad \sum_{k\in\mathcal{K}} q_k \le P_{\max}, \quad (24b)$$

$$q_k \ge \Upsilon_k, \quad (24c)$$

where $R_{k,1}^*$ and $R_{k,2}^*$ are the results of substituting $p_{k,1}^*$ and $p_{k,2}^*$ into $R_{k,1}'$ and $R_{k,2}'$, respectively, and

$$R_{k,1}^* = \log_2\left(1+\frac{\left|h_{k,1}\right|^2 q_k}{2^{R_{k,2}^{\min}}\sigma^2} + \frac{\left|h_{k,1}\right|^2}{2^{R_{k,2}^{\min}}\left|h_{k,2}\right|^2} - \frac{\left|h_{k,1}\right|^2}{\left|h_{k,2}\right|^2}\right), \quad (25a)$$

$$R_{k,2}^* = R_{k,2}^{\min}. \quad (25b)$$

Note that (24) is still a non-convex problem due to its fractional form. Nevertheless, it is easily seen that the numerator of (24) is a concave function with respect to q_k, and the denominator of (24) is a convex function with respect to q_k. Thus, (24) is a concave-convex fractional optimization problem, and it can be associated with the following parametric problem with a more tractable nonfractional form [40]:

$$\max_{\mathbf{q}} \ Q(\mathbf{q}) \triangleq R(\mathbf{q}) - \alpha P(\mathbf{q}) \quad (26a)$$

$$\text{s.t.} \ (24b) - (24c), \quad (26b)$$

where $R(\mathbf{q}) = \sum\limits_{k\in\mathcal{K}}\left(R_{k,1}^* + R_{k,2}^{\min}\right)$, $P(\mathbf{q}) = \frac{1}{\eta}\sum\limits_{k\in\mathcal{K}} q_k + P_c$ and α can be regarded as a scalar weight of $P(\mathbf{q})$, which can also be interpreted as a penalty of power consumption.

For a given α, the optimal solution of (26) is denoted by $\hat{\mathbf{q}}$. Let $\hat{\mathbf{q}}^*$ be the optimal solution of (24) and α^* be the maximum energy efficiency of (24), i.e., $\alpha^* = R(\hat{\mathbf{q}}^*)/P(\hat{\mathbf{q}}^*) = \max_{\mathbf{q}}\{R(\mathbf{q})/P(\mathbf{q})\}$. We define a function $F(\alpha)$ as

$$F(\alpha) \triangleq \max_{\mathbf{q}}\{R(\mathbf{q}) - \alpha P(\mathbf{q})\}. \quad (27)$$

It can be easily seen that solving (24) is equivalent to finding α^* such that

$$F(\alpha^*) = \max_{\mathbf{q}}\{R(\mathbf{q}) - \alpha^* P(\mathbf{q})\} = R(\hat{\mathbf{q}}^*) - \alpha^* P(\hat{\mathbf{q}}^*) = 0 \quad (28)$$

To find α^*, an iterative algorithm based on the Dinkelbach approach can be designed. In each iteration, with a given value of $\alpha^{(n)}$, we compute the power budget $\hat{\mathbf{q}}^{(n)}$ by solving the equivalent problem (26). Then, we update $\alpha^{(n+1)} = R\left(\hat{\mathbf{q}}^{(n)}\right)/P\left(\hat{\mathbf{q}}^{(n)}\right)$ for the obtained $\hat{\mathbf{q}}^{(n)}$. This iterative algorithm can guarantee to converge to the optimal value α^* if problem (26) can be solved in each iteration. Thus, the optimal solution $\hat{\mathbf{q}}^*$ to problem (24) can also be obtained. For this purpose, we first solve problem (26) with given α in the following analysis.

It is easy to prove that the optimization in (26) is a standard convex maximization problem. It can be shown that a strong duality holds and that the duality gap is zero, under some mild conditions. Hence, we can solve problem (26) by its associated dual. We denote the dual variables associated with the maximum power constraint by λ. Define $A_k = 1 + \frac{|h_{k,1}|^2}{2^{R_{k,2}^{\min}}|h_{k,2}|^2} - \frac{|h_{k,1}|^2}{|h_{k,2}|^2}$ and $B_k = \frac{|h_{k,1}|^2}{2^{R_{k,2}^{\min}}\sigma^2}$. The Lagrangian function of problem (26) can be written as

$$\begin{aligned} L(\mathbf{q},\lambda) &= \sum_{k\in\mathcal{K}}\left[\log_2(A_k + B_k q_k) + R_{k,2}^{\min}\right] \\ &\quad -\alpha\left(\frac{1}{\eta}\sum_{k\in\mathcal{K}} q_k + P_c\right) + \lambda\left(\sum_{k\in\mathcal{K}} q_k - P_{\max}\right) \\ &= \sum_{k\in\mathcal{K}} R_{k,2}^{\min} - \alpha P_c - \lambda P_{\max} + \Phi(\mathbf{q},\lambda), \end{aligned} \quad (29)$$

where

$$\Phi(\mathbf{q},\lambda) = \sum_{k\in\mathcal{K}}\left[\log_2(A_k + B_k q_k) - \frac{\alpha}{\eta}q_k + \lambda q_k\right]. \quad (30)$$

Since it is a convex problem and satisfies Slater's condition, thus the KKT conditions are necessary and sufficient to obtain the optimal solution. To obtain the optimal solution, KKT conditions (i.e., stationary condition, primal feasible condition, dual feasibility condition and complementary slackness condition) of problem (26) can be written as follows [41]:

Stationary condition:

$$-\frac{\partial Q}{\partial q_k} + \lambda = \frac{-B_k}{\ln 2(A_k + B_k q_k)} + \frac{\alpha}{\eta} + \lambda = 0 \quad (31)$$

Primal feasible condition:

$$\sum_{k\in\mathcal{K}} q_k - P_{\max} \le 0. \quad (32)$$

Dual feasibility condition: $\lambda \ge 0$.

Complementary slackness condition:

$$\lambda\left(\sum_{k\in\mathcal{K}} q_k - P_{\max}\right) = 0. \quad (33)$$

From (24c) and (31), we can derive the optimal solution to (26) as:

$$\hat{q}_k^* = \left[\frac{1}{\ln 2\left(\frac{\alpha}{\eta}+\lambda\right)} - \frac{A_k}{B_k}\right]_{\Upsilon_k}^{\infty}, \quad (34)$$

where $[x]_a^\infty = \max(x,a)$ and λ is chosen such that $\sum\limits_{k\in\mathcal{K}}\hat{q}_k^* = P_{\max}$ based on (33). We can give the following proof.

Proof: If $\lambda = 0$, from (31), we have $\frac{\partial Q}{\partial q_k} = 0$, which indicates that Q is a constant function with respect to q_k, i.e., $R(\mathbf{q}) - \alpha P(\mathbf{q}) = Y$. However, Q should be a concave function with respect to q_k. In this case, we can obtain $\lambda \neq 0$. Thus, from (33), λ is chosen such that $\sum\limits_{k\in\mathcal{K}} \hat{q}_k^* = P_{\max}$.

After the optimal solution to problem (26) is obtained, we can find an α^* such that $F(\alpha^*) = 0$. Thereby, the optimal power allocation in this STAR-RIS assisted MIMO-NOMA system is obtained.

B. Phase Shift Optimization

In this section, we focus on the phase shift optimization. Given by the precoding vectors $\mathbf{w}_k$ and power allocation $p_{k,1}^*$ and $p_{k,2}^*$ obtained from the beamforming optimization, the energy efficiency maximization problem (9) is rewritten as a sum-rate maximization problem, which is

$$\max_{\mathbf{\Theta}_n} \sum_{k\in\mathcal{K}}\sum_{j=1}^{2} R_{k,j} \tag{35a}$$

$$\text{s.t.}\quad R_{k,j} \geq R_{k,j}^{\min}, j = 1, 2, \tag{35b}$$

$$0 \leq \theta_m^n < 2\pi, m = 1, \ldots, M \tag{35c}$$

Note that (35) is not a convex problem because $R_{k,j}$ is not convex with respect to $\mathbf{\Theta}_n$. Therefore, we optimize the phase shift of the STAR-RIS by using SCA, which is widely used to approximate the non-convex problems into convex ones [37]. The main idea of SCA is to find out the problem whose optimal value is close to that of the original problem with iterations. Define a variable vector $\mathbf{d}_n = [d_1^n, \ldots, d_M^n]^H = \left[e^{j\theta_1^n}, \ldots, e^{j\theta_M^n}\right]^H$ and fixed vectors $\mathbf{a}_{j,l}^k = \Delta_{k,l}\sqrt{\beta_n}\text{diag}\left(\mathbf{v}_k^H \bar{\mathbf{h}}_{k,l}^H\right)\bar{\mathbf{G}}$ which $l \leq j$. Note the decoding order is assumed to be $(U_{k,2}, U_{k,1})$ in the k user pair in this paper. Besides, the inter-pair interference has been canceled by zero-forcing precoding in the last subsection. Thus, the SINR of $U_{k,2}$ decoded at l-th user in the k user pair can be expressed as

$$SINR_{2,l}^k = \frac{\left|\mathbf{d}_n^H \mathbf{a}_{2,l}^k \mathbf{w}_k\right|^2 p_{k,2}^*}{\left|\mathbf{d}_n^H \mathbf{a}_{2,l}^k \mathbf{w}_k\right|^2 p_{k,1}^* + \sigma^2}. \tag{36}$$

The SINR of $U_{k,1}$ decoded at itself can be expressed as

$$SINR_1^k = \frac{\left|\mathbf{d}_n^H \mathbf{a}_{1,1}^k \mathbf{w}_k\right|^2 p_{k,1}^*}{\sigma^2}. \tag{37}$$

Note both (35a) and (35b) in (35) are non-convex. Thus, in order to solve (35) effectively, we first propose to make (35a) convex. Define a slack variable b such that

$$\sum_{k\in\mathcal{K}}\sum_{j=1}^{2} R_{k,j} \geq b. \tag{38}$$

Based on the transformation, constraint (38) is still not convex. Thus, we further introduce a new vector $\mathbf{e}_k = [e_{k,1}, e_{k,2}]$ to equvalently transform (38) to

$$\sum_{k\in\mathcal{K}}\sum_{j=1}^{2} \log_2(e_{k,j}) \geq b, \tag{39a}$$

$$1 + SINR_{j,l}^k \geq e_{k,j}. \tag{39b}$$

Subsequently, we use another variable vector named $\mu_k = [\mu_{k,1}, \mu_{k,2}]$ to transform constraint (39a) to convex form, which can be rewritten as

$$\sum_{k\in\mathcal{K}}\sum_{j=1}^{2} \mu_{k,j} \geq b, \tag{40a}$$

$$e_{k,j} \geq 2^{\mu_{k,j}}. \tag{40b}$$

Now, the relationship between these slack variables introduced based on (38), (39a), (40a) and (40b) can be summrized as

$$\sum_{k\in\mathcal{K}}\sum_{j=1}^{2} \log_2\left(1 + SINR_{j,l}^k\right) \geq \sum_{k\in\mathcal{K}}\sum_{j=1}^{2} \log_2(e_{k,j}) \geq \sum_{k\in\mathcal{K}}\sum_{j=1}^{2} \mu_{k,j} \geq b. \tag{41}$$

Considering the expression of SINR is a form of fraction, it is alternative to introduce a series of variables with the form of $\varphi_{j,l}^k$, where $l \leq j$, to rewrite the SINR in (39b) as

$$\left|\mathbf{d}_n^H \mathbf{a}_{j,l}^k \mathbf{w}_k\right|^2 \geq (e_{k,j} - 1)\frac{\varphi_{j,l}^k}{p_{k,j}^*}, \tag{42a}$$

$$\left|\mathbf{d}_n^H \mathbf{a}_{j,l}^k \mathbf{w}_k\right|^2 p_{k,1}^* + \sigma^2 \leq \varphi_{j,l}^k. \tag{42b}$$

For the case $j = l = 1$, the expression should be written as

$$\left|\mathbf{d}_n^H \mathbf{a}_{1,1}^k \mathbf{w}_k\right|^2 \geq (e_{k,1} - 1)\frac{\varphi_{1,1}^k}{p_{k,1}^*}, \tag{43a}$$

$$\sigma^2 \leq \varphi_{1,1}^k. \tag{43b}$$

In the following, our aim is to convert (42a) to a convex form. Firstly, we introduce a series of variables $f_{j,l}^{k,\mathrm{Re}}$ and $f_{j,l}^{k,\mathrm{Im}}$ which denote the real part and the imaginary part of $\mathbf{d}_n^H \mathbf{a}_{j,l}^k \mathbf{w}_k$. Thus, $f_{j,l}^{k,\mathrm{Re}}$ and $f_{j,l}^{k,\mathrm{Im}}$ can be expressed as

$$f_{j,l}^{k,\mathrm{Re}} = \Re\left\{\mathbf{d}_n^H \mathbf{a}_{j,l}^k \mathbf{w}_k\right\}, \tag{44a}$$

$$f_{j,l}^{k,\mathrm{Im}} = \Im\left\{\mathbf{d}_n^H \mathbf{a}_{j,l}^k \mathbf{w}_k\right\}. \tag{44b}$$

Note (44a) and (44b) are convex constraints. Although (43a) is still non-convex constarint, instead of introducing new slack variables, SCA is applied to deal with this non-convex constraint. The main idea of SCA is to use the First-order Taylor approximation to convert the non-convex functions to affine [42].

In this paper, the constraint (42a) can be approximated to affine functions by applying SCA, which can be expressed as [37]

$$\begin{aligned}&\left(\left(f_{j,l}^{k,\mathrm{Re}}\right)^{(t)}\right)^2+\left(\left(f_{j,l}^{k,\mathrm{Im}}\right)^{(t)}\right)^2\\&+2\left(f_{j,l}^{k,\mathrm{Re}}\right)^{(t)}\left(f_{j,l}^{k,\mathrm{Re}}-\left(f_{j,l}^{k,\mathrm{Re}}\right)^{(t)}\right)\\&+2\left(f_{j,l}^{k,\mathrm{Im}}\right)^{(t)}\left(f_{j,l}^{k,\mathrm{Im}}-\left(f_{j,l}^{k,\mathrm{Im}}\right)^{(t)}\right)\\&\geq\left(\left(e_{k,j}\right)^{(t)}-1\right)\left(\frac{\varphi_{j,l}^{k}}{p_{k,j}^{*}}\right)^{(t)}+\left(\frac{\varphi_{j,l}^{k}}{p_{k,j}^{*}}\right)^{(t)}\left(e_{k,j}-\left(e_{k,j}\right)^{(t)}\right)\\&+\frac{\left(\left(e_{k,j}\right)^{(t)}-1\right)}{p_{k,j}^{*}}\left(\frac{\varphi_{j,l}^{k}}{p_{k,j}^{*}}-\left(\frac{\varphi_{j,l}^{k}}{p_{k,j}^{*}}\right)^{(t)}\right),\end{aligned}\tag{45}$$

where t represents the t-th iteration. As the number of iterations grows, the value of $\left(f_{j,l}^{k,\mathrm{Re}}\right)^{(t)}$ and $\left(f_{j,l}^{k,\mathrm{IM}}\right)^{(t)}$ will be close to the value of $f_{j,l}^{k,\mathrm{Re}}$ and $f_{j,l}^{k,\mathrm{Im}}$, leading to the scaled value is very close to the original value. Thus, the result will be more and more approached to the optimal. Then, we explore the convexity of the QoS constraint (35b). Apparently, it is obvious to find that (35b) is non-convex in terms of the expression directly. We rewrite this constraint as

$$\frac{\left|\mathbf{d}_n^H\mathbf{a}_{j,l}^k\mathbf{w}_k\right|^2}{\left|\mathbf{d}_n^H\mathbf{a}_{j,l}^k\mathbf{w}_k\right|^2p_{k,1}^*+\sigma^2}\geq\frac{2^{R_{k,j}^{\min}}-1}{p_{k,j}^*},\tag{46}$$

where $R_{k,j}^{\min}$ is a constant. After that, this constraint can be reformulated with SCA as

$$\begin{aligned}&\left(\left(f_{j,l}^{k,\mathrm{Re}}\right)^{(t)}\right)^2+\left(\left(f_{j,l}^{k,\mathrm{Im}}\right)^{(t)}\right)^2\\&\quad+2\left(f_{j,l}^{k,\mathrm{Re}}\right)^{(t)}\left(f_{j,l}^{k,\mathrm{Re}}-\left(f_{j,l}^{k,\mathrm{Re}}\right)^{(t)}\right)\\&\quad+2\left(f_{j,l}^{k,\mathrm{Im}}\right)^{(t)}\left(f_{j,l}^{k,\mathrm{Im}}-\left(f_{j,l}^{k,\mathrm{Im}}\right)^{(t)}\right)\\&\quad\geq\left(\frac{2^{R_{k,j}^{\min}}-1}{p_{k,j}^*}\right)\left(\left|\mathbf{d}_n^H\mathbf{a}_{j,l}^k\mathbf{w}_k\right|^2p_{k,1}^*+\sigma^2\right).\end{aligned}\tag{47}$$

Obviously, the constraint (47) is a convex set because it satisfies the form of Second-Order-Cone (SOC). Now, after the above transformation, the final form of this phase shift optimization can be expressed as

$$\max_{\mathbf{d}_n,b,\mathbf{e}_k,\mu_k,\varphi_k,f^{k,\mathrm{Re}},f^{k,\mathrm{Im}}}\ \mathrm{b}\tag{48a}$$
$$\mathrm{s.t.}\ (35c),(40b),(44a),(44b),(45),(47).\tag{48b}$$

Problem (48) is now convex, which can be solved directly by the optimization tool, e.g., CVX, in Matlab.

C. Algorithm Design

The details of the proposed alternating optimization algorithm are shown in Algorithm 1, in which problem (26) and problem (48) are alternatively solved until the convergence metric is triggered. Particularly, at each iteration, we firstly obtained the precoding matrix $\mathbf{w}_k^*\in\mathbb{C}^{N\times 1}$ and power allocation $p_{k,j}^*$ based on the Dinkelbach approach. Then, to guarantee the feasibility and convergence of Algorithm 1, we choose the initial optimized variables by evaluating the phase shift vectors and satisfying all the constraints. It is important to find the initial values since the convergence of the proposed SCA-based method is sensitive to the initial points. Specifically, we initialize $\mathbf{d}_k^{(0)}$ as $\mathbf{\Theta}_k^{(0)}$. Then $\mathbf{e}_k^{(0)}$, $\mu_k^{(0)}$, $\varphi_k^{(0)}$ and $b^{(0)}$ can be computed by replacing the inequalities of (39b), (40b), (42a) and (40a) with equalities. At each iteration, utilizing CVX tools, we solve problem (48) given by the values of the optimized variables by the last iteration. This process will terminate until its convergence with the tolerance.

Algorithm 1 Optimal Beamforming and Phase Shift Algorithm

1: Initialize $\mathbf{\Theta}_n^{(0)}$ and set the outer iteration number $t=1$.
2: **repeat**
3: **Beamforming Optimization:** Calculate precoding matrix $\mathbf{w}_k$ according to (13); Initialize $\alpha^{(0)}=0$, $F^{(0)}=\infty$ and precision $\delta>0$.
4: **While** $|F(\alpha)|>\delta$ **do**
5: Calculate $p_{k,j}^*$ according to (23);
6: Find the optimal $\hat{\mathbf{q}}^*$ according to (34);
7: Calculate $F(\alpha)$;
8: Update $\alpha=Q(\hat{\mathbf{q}}^*)$;
9: **output**: $p_{k,j}^*$, α and $\hat{\mathbf{q}}^*$.
10: **Phase shift Optimization:** Initialize $\mathbf{d}_n^{(0)}$, $\mathbf{e}_k^{(0)}$, $\mu_k^{(0)}$, $\varphi_k^{(0)}$, $b^{(0)}$, $\left(f^{k,\mathrm{Re}}\right)^{(0)}$, $\left(f^{k,\mathrm{Im}}\right)^{(0)}$ and precision $\delta>0$.
11: **While** $b^{(t)}-b^{(t-1)}>\delta$ **do**
12: Solve (48) to find $\mathbf{d}_n^{(t)}$ by SCA method.
13: **output**: $\mathbf{d}_n^{(t)}$ and $EE^{(t)}$.

IV. Simulation Results and Analysis

In this section, in order to verify the superior performance of our proposed joint optimization of the power allocation and the phase shift of STAR-RIS, we made a thorough comparison with the OMA based algorithms and the random phase shift algorithms. For simplicity, we first consider a simple scenario where there only exist one R user pair and one T user pair, i.e., $K=1$. Initially, we compared the performance of the proposed NOMA based scheme with OMA based scheme in both optimal and random phase shift under the same number of antennas ($N=4$). Note that in the OMA based schemes, the power allocation of users is optimized in a waterfilling manner. From the comparison between our proposed NOMA based optimal algorithms and the OMA based algorithms, we can demonstrate that our optimal power allocation mechanism outperforms the power allocation mechanism with waterfilling manner, as well as the effectiveness of NOMA. After demonstrating the superior performance of the proposed NOMA based scheme compared with the OMA based scheme, we also compare the proposed optimal algorithm with the random phase shift algorithm considering different number of antennas. Note that the beamforming optimization in the random phase shift scheme is the same

TABLE I
SIMULATION PARAMETERS

Parameter	Value
d	10 m
ρ_0	-30 dB
α_{BR}, α_{RU}	2.5
K_{BR}, K_{RU}	10
$\Gamma_{k,j}^{\min}$	-10 dB
σ^2	-60 dBm
M	50
P_c	0.01 W
P_{max}	0.1 W
η	0.8

as the proposed algorithm. It is worthwhile to point out that for the random phase shift schemes, there is no doubt that the random phase shifts would result the fluctuation of the energy efficiency performance. Nevertheless, what we cannot ignore is the impact of the growth of the value at x-axis on the trend of the energy efficiency value. Moreover, in order to alleviate the fluctuation of the energy efficiency value caused by the random phase shifts, we need to run the algorithms many times, normally no less than 500 times, and then calculate the average value of the output. In this case, the schemes with random phase shifts would have the same trend as the optimal phase shift schemes. In fact, we can see the same simulation setting in many other works related to RIS, such as [22] and [43]. Furthermore, in order to make our proposed algorithms cater for more realistic scenarios, we consider a more complicated system where $K = 2$. It is worthwhile to point out that the proposed algorithm can be utilized in large-scale communication scenarios with complex computing.

We consider that the distance between the BS and the STAR-RIS is 10 m. The distances of $U_{k,1}$ and $U_{k,2}$ from the STAR-RIS are randomly obtained in 10 to 20 m, and ensure that the distance between $U_{k,1}$ and the STAR-RIS is smaller than the distance between $U_{k,2}$ and the STAR-RIS. The channels from the BS to the STAR-RIS and from the STAR-RIS to the users are Rician fading channels. We set $\rho_0 = -30$ dB, $\alpha_{BR} = \alpha_{RU} = 2.5$, $K_{BR} = K_{RU} = 10$. Without the loss of generality, the minimal SINR requirement for all users is -10 dB and the additive white Gaussian noise σ^2 is -60 dBm. The other parameters in simulations are set as in Table I.

Fig. 2 describes the convergence process of the Dinkelbach approach. It is shown from Fig. 2 that the Dinkelbach approach can guarantee to converge to the optimal value after several iterations, which validates that the optimal precoding matrix $\mathbf{w}_k^*$ and power allocation $p_{k,j}^*$ can always be obtained. Besides, Fig. 2 also shows that an increasing number of antennas can contribute to a higher performance of energy efficiency.

In the next subsections, we first compare our proposed algorithm with OMA scheme in the scenario of the same number of antennas. Then, we make the comparison of our optimal algorithm with the random phase shift algorithm when the number of system antennas is different.

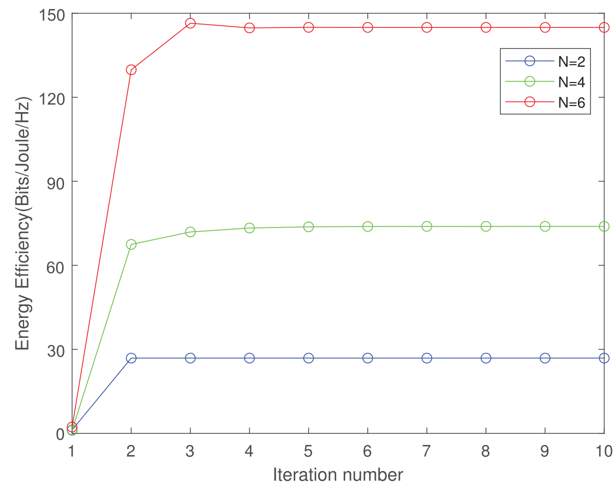

Fig. 2. The convergence of Dinkelbach approach.

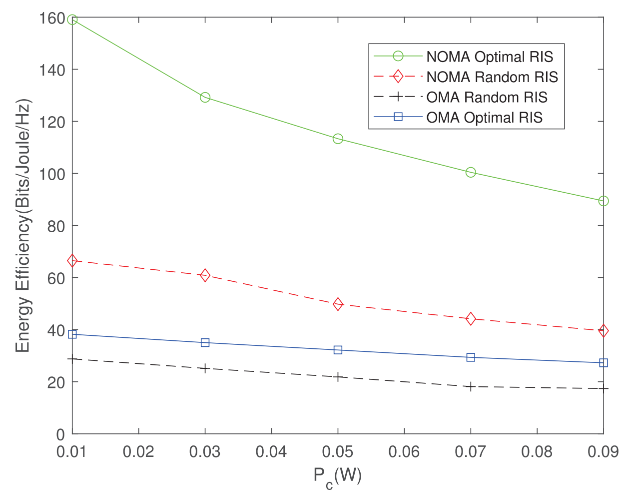

Fig. 3. EE versus the circuit power P_c.

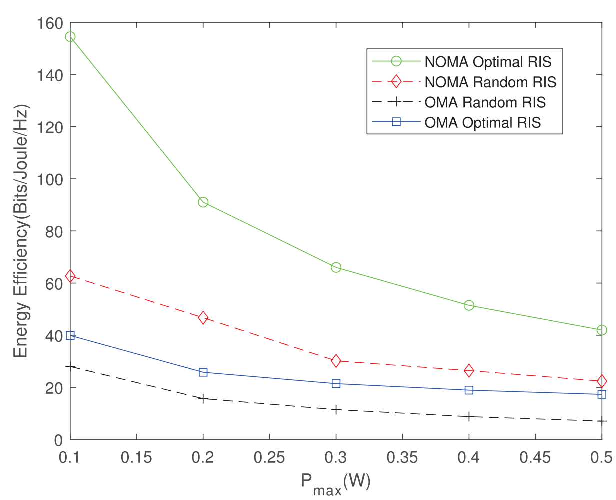

Fig. 4. EE versus the maximum power $P_{\max}$.

A. Comparison With OMA Scheme

In Fig. 3 and Fig. 4, we compare the performance of our proposed optimal NOMA based scheme with OMA based scheme in both optimal and random phase shift of the STAR-RIS. Note in the OMA scheme, the power allocation of users is optimized in a waterfilling manner. In Fig. 3, we can see the

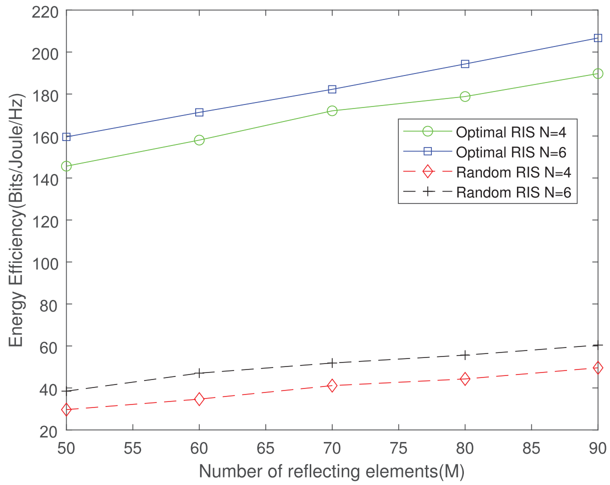

Fig. 5. EE versus the number of reflecting elements M.

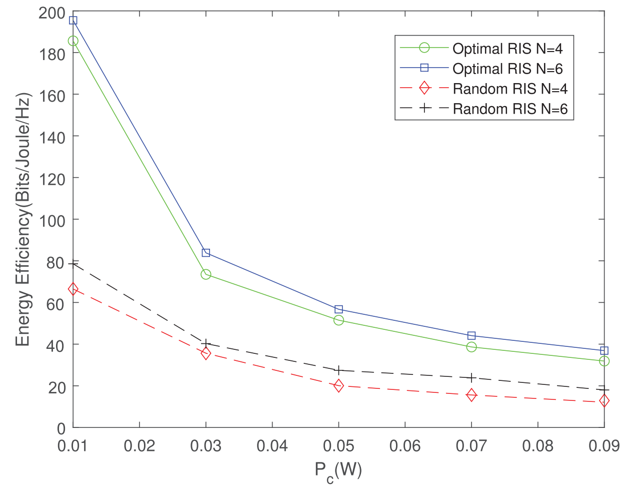

Fig. 6. EE versus the circuit power P_c.

relationship between energy efficiency and the circuit power P_c. As P_c increases, the energy efficiency decreases in all four schemes, which is determined by the definition of the energy efficiency. It is clearly seen that the NOMA scheme is better than the OMA scheme in terms of energy efficiency in our considered system. Note that even the energy efficiency performance of the OMA based scheme with optimal phase shift still worse than that of the NOMA based scheme with random phase shift, which validates the superiority of NOMA technology in improving energy efficiency. We can still find that our optimal phase shift algorithm is much better than the random phase shift algorithm in both NOMA and OMA, which verifies the effectiveness of our joint optimization algorithm.

Fig. 4 shows the energy efficiency performance versus the maximum power $P_{\max}$ for above four algorithms. We can witness that as $P_{\max}$ increases, the system energy efficiency decreases rapidly and gradually. This is determined by the relationship of increasing sum rate and increasing system energy consumption when $P_{\max}$ increases. When $P_{\max}$ is small, as $P_{\max}$ increases, the increasing system energy consumption dominates the energy efficiency performance, leading to the decrease of the energy efficiency value. As $P_{\max}$ further increases, the increasing system sum rate gradually dominates the system energy efficiency, causing the energy efficiency to decrease more slowly. In Fig. 4, we can see that the energy efficiency performance of our proposed NOMA based scheme with optimal phase shift is much better than that of NOMA based scheme with random phase shift, which shows the effectiveness of joint optimization of power allocation and phase shift of the STAR-RIS. Moreover, the NOMA based schemes can realize better energy efficiency performance compared with the OMA based schemes, which validates the effectiveness of NOMA in improving energy efficiency compared OMA in the proposed system.

B. Comparison With Random Phase Scheme ($K = 1$)

Fig. 5 shows the relationship between energy efficiency and the number of the reflecting elements of the STAR-RIS. For a comprehensive comparison, two different numbers of the antennas are selected in the proposed algorithm to compare their energy efficiency values with those with random phase shifts. Initially, it can be seen that the energy efficiency values optimized by the proposed algorithm are much higher than those with random phase shifts. Also, the performance of energy efficiency of schemes with 6 antennas is better than those with only 4 antennas. Besides, it can also be found that the figure of the energy efficiency increases as M grows. The performance keeps improving, but the improvement becomes smaller when the number of reflecting elements increases. This is because the feasible domain of each channel between antennas is narrowed down by increasing M due to the fixed $P_{\max}$.

Fig. 6 shows the energy efficiency performance versus the circuit power P_c at the BS. From the figures under both optimized and random phase shifts circumstances, it can be seen that the energy efficiency values decreases when the circuit power increases. According to the definition of energy efficiency, its value will becomes smaller when P_c increases. Nevertheless, the slope of the decreasing curve gets smaller with P_c, which is because that the optimization dominates in increasing system energy efficiency when P_c is small. It can also be observed that energy efficiency of the proposed scheme always outperforms that of the random phase shifts scheme, as well as the performance of energy efficiency of schemes with 6 antennas is always better than those with only 4 antennas.

Fig. 7 shows the the energy efficiency performance of different resource allocation strategies versus maximum transmitted power $P_{\max}$. We can see that, as $P_{\max}$ increasing, the energy efficiency first declines rapidly and then slowly. This is because although an increasing $P_{\max}$ can contribute to higher transmit power of both two users in a pair, which derives higher sum rate in the system, the power consumption also increases in this case. In such a MIMO-NOMA network, when $P_{\max}$ is small, the increasing power consumption dominates the impact on the system energy efficiency, which leads to the rapid decrease of the system energy efficiency at the very beginning. As $P_{\max}$ increases, the increasing sum rate

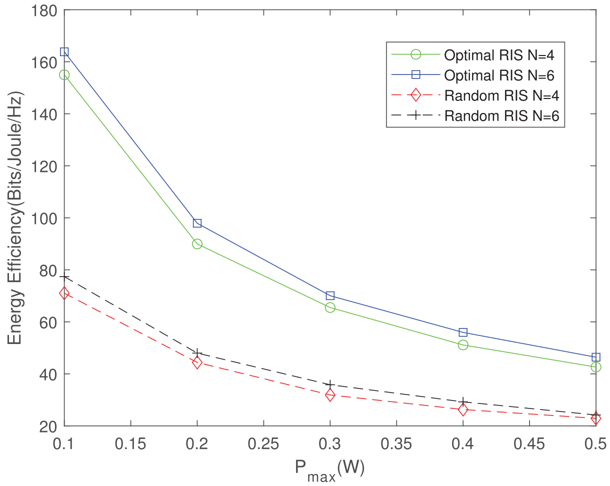

Fig. 7. EE versus the maximum power $P_{\max}$.

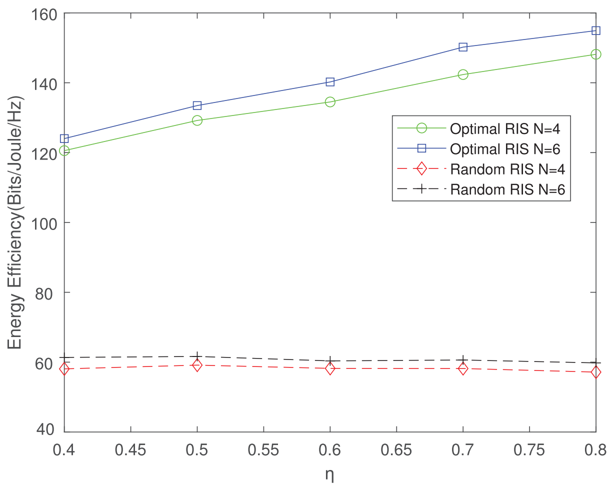

Fig. 8. EE versus power amplifier coefficient η.

dominates the performance of energy efficiency, leading to the gradual decrease of the system energy efficiency. Besides, we also find that the proposed algorithm outperforms the random phase shift algorithm and the greater the number of antennas for both users and BS, the greater the energy efficiency.

Fig. 8 shows the relationship between energy efficiency and the power amplifier coefficient. From the curve, it can be observed that the energy efficiency can increase as the value of η increases in the proposed scheme. Moreover, the energy efficiency of proposed algorithm with 6 antennas outperforms that with 4 antennas, which demonstrates the effectiveness of MIMO. Nevertheless, we can find that the energy efficiency of random phase shift algorithm fluctuates with the increase of η. It is because the random phase shift dominates the performance of energy efficiency in such a random algorithm. We also get that the proposed algorithm can achieve a better performance compared with the random phase shift algorithm.

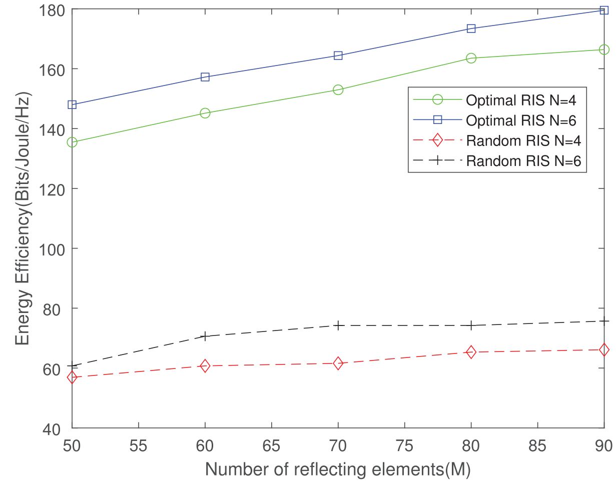

Fig. 9. EE versus the number of reflecting elements $M(K = 2)$.

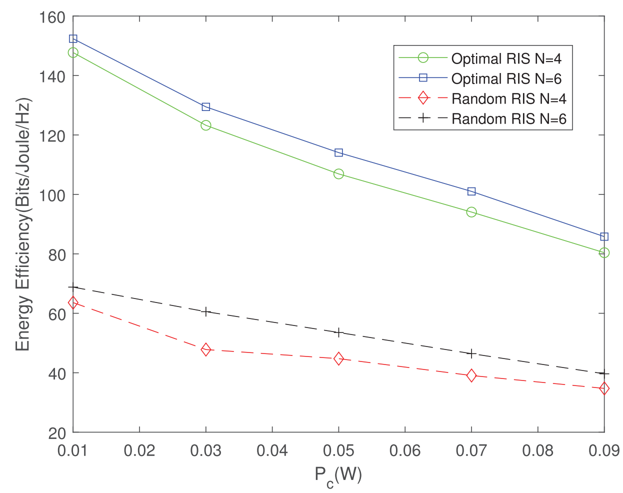

Fig. 10. EE versus the circuit power $P_c(K = 2)$.

C. Comparison With Random Phase Scheme ($K = 2$)

It can be observed from Fig. 9 that when $K = 2$, the energy efficiency still increases with the growth of number of reflecting elements M, which is the same as in Fig. 5. As M increases, the improvement of energy efficiency becomes smaller, which is because the feasible domain of each channel between antennas is narrowed down by increasing M due to the fixed $P_{\max}$. Besides, we also find that the energy efficiency in Fig. 9 is smaller than that in Fig. 5. This is because the increasing number of user pairs would contribute to higher transmitting power. Moreover, the proposed algorithm has a higher energy efficiency compared with the random algorithm, and as the number of antennas increases, the energy efficiency increases. These findings demonstrate the effectiveness of the proposed optimal algorithm.

Fig. 10 shows the relationship between energy efficiency and the circuit power P_c in a more complex scenario where $K = 2$. Under this circumstance, we find that the same trend as in Fig. 6 can be achieved, i.e., as P_c increases, the energy efficiency performance of both the proposed algorithm and the random algorithm decreases. Our optimal algorithm still outperforms the random phase shift algorithm, and an increasing number of antennas can lead to better energy efficiency performance. Moreover, compared with Fig. 6, the energy efficiency becomes smaller, which is because as the number of user pairs increases, to meet the QoS of all of users, larger transmitting power is also required.

V. Conclusion

In this paper, we designed an algorithm to maximize the energy efficiency in a STAR-RIS assisted MIMO-NOMA system with multiple user pairs. Specifically, due to the non-convexity, we decoupled the primal problem into two subproblems, i.e., beamforming and phase shift optimization subproblems. By alternately optimizing the beamforming vectors and phase shifts of STAR-RIS, the optimal energy efficiency could be obtained through the proposed iterative algorithm. To decompose MIMO-NOMA channels into single-antenna NOMA channels in the system, we initially proposed to utilize signal alignment and zero-forcing methods, which simplifies the system implementation significantly. A more tractable beamforming optimization problem was obtained through Dinkelbach method as well as dual decomposition theories. SCA was also applied as a mathematical tool to convert some non-convex constraints to convex in the phase shift optimization problem. Simulation results verified the effectiveness of the proposed algorithm. Note that this work can also be addressed by machine learning, which will be considered in our future work.

References

[1] M. D. Renzo et al., "Smart radio environments empowered by AI reconfigurable meta-surfaces: An idea whose time has come," *EURASIP J. Wireless Commun. Netw.*, vol. 2019, pp. 1–20, May 2019.

[2] Q. Wu and R. Zhang, "Intelligent reflecting surface enhanced wireless network via joint active and passive beamforming," *IEEE Trans. Wireless Commun.*, vol. 18, no. 11, pp. 5394–5409, Nov. 2019.

[3] C. Pan et al., "Reconfigurable intelligent surfaces for 6G systems: Principles, applications, and research directions," *IEEE Commun. Mag.*, vol. 59, no. 6, pp. 14–20, Jun. 2021.

[4] Y. Liu et al., "STAR: Simultaneous transmission and reflection for 360° coverage by intelligent surfaces," *IEEE Wireless Commun.*, vol. 28, no. 6, pp. 102–109, Dec. 2021.

[5] J. Xu, Y. Liu, X. Mu, and O. A. Dobre, "STAR-RISs: Simultaneous transmitting and reflecting reconfigurable intelligent surfaces," 2021, *arXiv:2101.09663*.

[6] Z. Ding, X. Lei, G. K. Karagiannidis, R. Schober, J. Yuan, and V. Bhargava, "A survey on non-orthogonal multiple access for 5G networks: Research challenges and future trends," *IEEE J. Sel. Areas Commun.*, vol. 35, no. 10, pp. 2181–2195, Oct. 2017.

[7] Y. Liu, Z. Qin, M. Elkashlan, Z. Ding, A. Nallanathan, and L. Hanzo, "Nonorthogonal multiple access for 5G and beyond," *Proc. IEEE*, vol. 105, no. 12, pp. 2347–2381, Dec. 2017.

[8] Z. Ding et al., "A state-of-the-art survey on reconfigurable intelligent surface assisted non-orthogonal multiple access networks," *Proc. IEEE*, vol. 110, no. 9, pp. 1358–1379, Sep. 2022.

[9] B. Zheng, Q. Wu, and R. Zhang, "Intelligent reflecting surface-assisted multiple access with user pairing: NOMA or OMA?" *IEEE Commun. Lett.*, vol. 24, no. 4, pp. 753–757, Apr. 2020.

[10] J. Zhu, Y. Huang, J. Wang, K. Navaie, and Z. Ding, "Power efficient IRS-assisted NOMA," *IEEE Trans. Commun.*, vol. 69, no. 2, pp. 900–913, Feb. 2021.

[11] X. Xie, F. Fang, and Z. Ding, "Joint optimization of beamforming, phase-shifting and power allocation in a multi-cluster IRS-NOMA network," *IEEE Trans. Veh. Technol.*, vol. 70, no. 8, pp. 7705–7717, Aug. 2021.

[12] J. Zuo, Y. Liu, Z. Qin, and N. Al-Dhahir, "Resource allocation in intelligent reflecting surface assisted NOMA systems," *IEEE Trans. Commun.*, vol. 68, no. 11, pp. 7170–7183, Nov. 2020.

[13] Q. Wu, X. Zhou, and R. Schober, "IRS-assisted wireless powered NOMA: Do we really need different phase shifts in DL and UL?" *IEEE Wireless Commun. Lett.*, vol. 10, no. 7, pp. 1493–1497, Jul. 2021.

[14] X. Mu, Y. Liu, L. Guo, J. Lin, and N. Al-Dhahir, "Exploiting intelligent reflecting surfaces in NOMA networks: Joint beamforming optimization," *IEEE Trans. Wireless Commun.*, vol. 19, no. 10, pp. 6884–6898, Oct. 2020.

[15] B. Di, H. Zhang, L. Song, Y. Li, Z. Han, and H. V. Poor, "Hybrid beamforming for reconfigurable intelligent surface based multi-user communications: Achievable rates with limited discrete phase shifts," *IEEE J. Sel. Areas Commun.*, vol. 38, no. 8, pp. 1809–1822, Aug. 2020.

[16] F. Fang, Y. Xu, Q.-V. Pham, and Z. Ding, "Energy-efficient design of IRS-NOMA networks," *IEEE Trans. Veh. Technol.*, vol. 69, no. 11, pp. 14088–14092, Nov. 2020.

[17] Z. Li et al., "Energy efficient reconfigurable intelligent surface enabled mobile edge computing networks with NOMA," *IEEE Trans. Cogn. Commun. Netw.*, vol. 7, no. 2, pp. 427–440, Jun. 2021.

[18] F. Fang, H. Zhang, J. Cheng, and V. C. M. Leung, "Energy-efficient resource allocation for downlink non-orthogonal multiple access network," *IEEE Trans. Commun.*, vol. 64, no. 9, pp. 3722–3732, Sep. 2016.

[19] X. Gao, Y. Liu, X. Liu, and L. Song, "Machine learning empowered resource allocation in IRS aided MISO-NOMA networks," 2021, *arXiv:2103.11791*.

[20] Z. Yang, Y. Liu, Y. Chen, and N. Al-Dhahir, "Machine learning for user partitioning and phase shifters design in RIS-Aided NOMA networks," *IEEE Trans. Commun.*, vol. 69, no. 11, pp. 7414–7428, Nov. 2021.

[21] M. Shehab, B. S. Ciftler, T. Khattab, M. M. Abdallah, and D. Trinchero, "Deep reinforcement learning powered IRS-assisted downlink NOMA," *IEEE Open J. Commun. Soc.*, vol. 3, pp. 729–739, 2022.

[22] J. Zuo, Y. Liu, E. Basar, and O. A. Dobre, "Intelligent reflecting surface enhanced millimeter-wave NOMA systems," *IEEE Commun. Lett.*, vol. 24, no. 11, pp. 2632–2636, Nov. 2020.

[23] P. Liu, Y. Li, W. Cheng, X. Gao, and X. Huang, "Intelligent reflecting surface aided NOMA for millimeter-wave massive MIMO with lens antenna array," *IEEE Trans. Veh. Technol.*, vol. 70, no. 5, pp. 4419–4434, May 2021.

[24] A. S. de Sena et al., "IRS-assisted massive MIMO-NOMA networks: Exploiting wave polarization," *IEEE Trans. Wireless Commun.*, vol. 20, no. 11, pp. 7166–7183, Nov. 2021.

[25] S. Jiao, F. Fang, X. Zhou, and H. Zhang, "Joint beamforming and phase shift design in downlink UAV networks with IRS-assisted NOMA," *J. Commun. Inf. Netw.*, vol. 5, no. 2, pp. 138–149, Jun. 2020.

[26] S. Zhang, H. Zhang, B. Di, Y. Tan, Z. Han, and L. Song, "Beyond intelligent reflecting surfaces: Reflective-transmissive metasurface aided communications for full-dimensional coverage extension," *IEEE Trans. Veh. Technol.*, vol. 69, no. 11, pp. 13905–13909, Nov. 2020.

[27] Y. Zhang, B. Di, H. Zhang, Z. Han, H. V. Poor, and L. Song, "Meta-wall: Intelligent omni-surfaces aided multi-cell MIMO communications," *IEEE Trans. Wireless Commun.*, vol. 21, no. 9, pp. 7026–7039, Sep. 2022.

[28] X. Mu, Y. Liu, L. Guo, J. Lin, and R. Schober, "Simultaneously transmitting and reflecting (STAR) RIS aided wireless communications," *IEEE Trans. Wireless Commun.*, vol. 21, no. 5, pp. 3083–3098, May 2022.

[29] C. Wu, X. Mu, Y. Liu, X. Gu, and X. Wang, "Resource allocation in STAR-RIS-Aided networks: OMA and NOMA," *IEEE Trans. Wireless Commun.*, vol. 21, no. 9, pp. 7653–7667, Sep. 2022.

[30] J. Zuo, Y. Liu, Z. Ding, L. Song, and H. Vincent Poor, "Joint design for simultaneously transmitting and reflecting (STAR) RIS assisted NOMA systems," 2021, *arXiv:2106.03001*.

[31] Y. Guo, F. Fang, D. Cai, and Z. Ding, "Energy-efficient design for a NOMA assisted STAR-RIS network with deep reinforcement learning," 2021, *arXiv:2111.15464*.

[32] Y. Li, M. Jiang, Q. Zhang, Q. Li, and J. Qin, "Cooperative non-orthogonal multiple access in multiple-input-multiple-output channels," *IEEE Trans. Wireless Commun.*, vol. 17, no. 3, pp. 2068–2079, Mar. 2018.

[33] Z. Ding, F. Adachi, and H. V. Poor, "The application of MIMO to non-orthogonal multiple access," *IEEE Trans. Wireless Commun.*, vol. 15, no. 1, pp. 537–552, Jan. 2016.

[34] Z. Ding, M. Peng, and H. V. Poor, "Cooperative non-orthogonal multiple access in 5G systems," *IEEE Commun. Lett.*, vol. 19, no. 8, pp. 1462–1465, Aug. 2015.

[35] Z. Ding, R. Schober, and H. V. Poor, "A general MIMO framework for NOMA downlink and uplink transmission based on signal alignment," *IEEE Trans. Wireless Commun.*, vol. 15, no. 6, pp. 4438–4454, Jun. 2016.

[36] Z. Chen, Z. Ding, X. Dai, and G. K. Karagiannidis, "On the application of quasi-degradation to MISO-NOMA downlink," *IEEE Trans. Signal Process.*, vol. 64, no. 23, pp. 6174–6189, Dec. 2016.

[37] T. Wang, F. Fang, and Z. Ding, "An SCA and relaxation based energy efficiency optimization for multi-user RIS-assisted NOMA networks," *IEEE Trans. Veh. Technol.*, vol. 71, no. 6, pp. 6843–6847, Jun. 2022.

[38] M. Zeng, E. Bedeer, O. A. Dobre, P. Fortier, Q.-V. Pham, and W. Hao, "Energy-efficient resource allocation for IRS-assisted multi-antenna uplink systems," *IEEE Wireless Commun. Lett.*, vol. 10, no. 6, pp. 1261–1265, Jun. 2021.

[39] J. Zhu, J. Wang, Y. Huang, S. He, X. You, and L. Yang, "On optimal power allocation for downlink non-orthogonal multiple access systems," *IEEE J. Sel. Areas Commun.*, vol. 35, no. 12, pp. 2744–2757, Dec. 2017.

[40] X. Wang, F.-C. Zheng, P. Zhu, and X. You, "Energy-efficient resource allocation in coordinated downlink multicell OFDMA systems," *IEEE Trans. Veh. Technol.*, vol. 65, no. 3, pp. 1395–1408, Mar. 2015.

[41] F. Fang, Y. Xu, Z. Ding, C. Shen, M. Peng, and G. K. Karagiannidis, "Optimal resource allocation for delay minimization in NOMA-MEC networks," *IEEE Trans. Commun.*, vol. 68, no. 12, pp. 7867–7881, Dec. 2020.

[42] B. Fang, Z. Qian, W. Zhong, and W. Shao, "Iterative precoding for MIMO wiretap channels using successive convex approximation," in *Proc. IEEE 4th Asia–Pacific Conf. Antennas Propag. (APCAP)*, Jun. 2015, pp. 65–66.

[43] S. Zargari, A. Khalili, and R. Zhang, "Energy efficiency maximization via joint active and passive beamforming design for multiuser MISO IRS-aided SWIPT," *IEEE Wireless Commun. Lett.*, vol. 10, no. 3, pp. 557–561, Mar. 2021.

Fang Fang (Member, IEEE) received the Ph.D. degree in electrical engineering from the University of British Columbia (UBC), Canada, in 2017. She is currently an Assistant Professor at the Department of Electrical and Computer Engineering and the Department of Computer Science, Western University, Canada. Prior to joining Western, she was an Assistant Professor at the Department of Engineering, Durham University, U.K., from 2020 to 2022. From 2018 to 2020, she was a Research Associate with the Department of Electrical and Electronic Engineering, The University of Manchester, U.K. Her current research interests include machine learning for intelligent wireless communications, non-orthogonal multiple access (NOMA), reconfigurable intelligent surface (RIS), multi-access edge computing (MEC), edge AI, and blockchain. She has been serving as a Technical Program Committee (TPC) Member for IEEE flagship conferences, such as, IEEE Globecom, IEEE ICC, and IEEE VTC. She received the Exemplary Reviewer Certificates of the IEEE Transactions on Communications in 2021 and 2017. She is currently an Associate Editor of IEEE Open Journal of the Communications Society.

Bibo Wu is currently pursuing the M.A.Eng. degree with the School of Microelectronics and Communication Engineering, Chongqing University of China, Chongqing, China. His main research interests include resource management in the integrated terrestrial-satellite relay networks, intelligent reflecting surface (IRS), and non-orthogonal multiple access (NOMA).

Shu Fu (Member, IEEE) received the Ph.D. degree in communication and information system from the University of Electronic Science and Technology of China, Chengdu, China, in 2016, focusing on cooperative multipoint (CoMP) wireless network, joint scheduling and routing in wavelength division multiplexing (WDM) network, and cross-network energy efficiency. He is currently an Associate Professor with the College of Communication Engineering, Chongqing University, Chongqing, China. His research interests include machine learning in B5G, UAV aided wireless networks, and terrestrial-satellite networks.

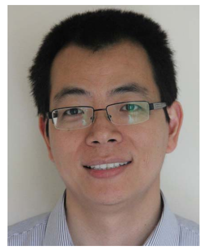

Zhiguo Ding (Fellow, IEEE) received the B.Eng. degree from the Beijing University of Posts and Telecommunications in 2000 and the Ph.D. degree from the Imperial College London in 2005. From July 2005 to April 2018, he was working with Queen's University Belfast, Imperial College London, Newcastle University, and Lancaster University. From October 2012 to September 2021, he was an Academic Visitor with Princeton University. Since April 2018, he has been with The University of Manchester, as a Professor of communications. His research interests are 5G networks, game theory, cooperative and energy harvesting networks, and statistical signal processing. He has received the EU Marie Curie Fellowship 2012–2014, the Top IEEE Transactions on Vehicular Technology Editor 2017, the IEEE Heinrich Hertz Award 2018, the IEEE Jack Neubauer Memorial Award 2018, the Best IEEE Signal Processing Letter Award 2018, and the Friedrich Wilhelm Bessel Research Award 2020. He was the Editor of IEEE Wireless Communications Letters, IEEE Transactions on Communications, and IEEE Communication Letters from 2013 to 2016. He is serving as an Area Editor for IEEE Open Journal of the Communications Society and the Editor for IEEE Transactions on Vehicular Technology. He is also a Distinguished Lecturer of IEEE ComSoc and a Web of Science Highly Cited Researcher in two categories 2021.

Xianbin Wang (Fellow, IEEE) received the Ph.D. degree in electrical and computer engineering from the National University of Singapore in 2001.

He is a Professor and the Tier-1 Canada Research Chair at Western University, Canada. Prior to joining Western, he was with the Communications Research Centre, Canada, as a Research Scientist/a Senior Research Scientist, from July 2002 to December 2007. From January 2001 to July 2002, he was a System Designer at STMicroelectronics. He has over 500 highly cited journal and conference papers, in addition to 30 granted and pending patents and several standard contributions. His current research interests include 5G/6G technologies, the Internet of Things, communications security, machine learning, and intelligent communications.

Dr. Wang is a fellow of the Canadian Academy of Engineering and the Engineering Institute of Canada. He has received many prestigious awards and recognitions, including the IEEE Canada R. A. Fessenden Award, the Canada Research Chair, the Engineering Research Excellence Award from Western University, the Canadian Federal Government Public Service Award, the Ontario Early Researcher Award, and the six IEEE Best Paper Awards. He was involved in many IEEE conferences including GLOBECOM, ICC, VTC, PIMRC, WCNC, CCECE, and CWIT, in different roles such as the General Chair, the Symposium Chair, a Tutorial Instructor, the Track Chair, the Session Chair, the TPC Co-Chair, and a keynote speaker. He was the Chair of IEEE ComSoc Signal Processing and Computing for Communications (SPCC) Technical Committee. He is currently serving as the Central Area Chair for IEEE Canada. He currently serves/has served as the editor-in-chief, the associate editor-in-chief, the editor/an associate editor for over ten journals. He has been nominated as an IEEE Distinguished Lecturer several times during the last ten years. He is an IEEE Distinguished Lecturer.